Digital Object Identifier 10.1109/ACCESS.2023.DOI

# **Practical X-ray Gastric Cancer Screening Using Refined Stochastic Data Augmentation and Hard Boundary Box Training**

### HIDEAKI OKAMOTO 1, TAKAKIYO NOMURA2, KAZUHITO NABESHIMA2, JUN HASHIMOTO2, AND HITOSHI IYATOMI1 (Member, IEEE)

Department of Applied Informatics, Graduate School of Science and Engineering, Hosei University, Tokyo, 184-8584 Japan

<sup>2</sup>Department of Radiology, Tokai University School of Medicine, Isehara

Corresponding author: Hitoshi Iyatomi (e-mail: iyatomi@hosei.ac.jp).

This study has been approved by the Institutional Review Board of Tokai University Hospital (No. 20R-033, date of approval: Jun. 12th,

**ABSTRACT** In gastric cancer screening, X-rays can be performed by radiographers, allowing them to see far more patients than endoscopy, which can only be performed by physicians. However, due to subsequent diagnostic difficulties, the sensitivity of gastric X-ray is only 85.5%, and little research has been done on automated diagnostic aids that directly target gastric cancer. This paper proposes a practical gastric cancer screening system for X-ray images taken under realistic clinical imaging conditions. Our system not only provides a diagnostic result for each image, but also provides an explanation for the result by displaying candidate cancer areas with bounding boxes. Training object detection models to do this was very expensive in terms of assigning supervised labels, and had the disadvantage of not being able to use negative (i.e., noncancer) data for training. Our proposal consists of two novel techniques: (1) refined stochastic gastric image augmentation (R-sGAIA) and (2) hard boundary box training (HBBT). The R-sGAIA probabilistically highlights the gastric folds in the X-ray image based on medical knowledge, thus increasing the detection efficiency of gastric cancer. The HBBT is a new, efficient, and versatile training method that can reduce the number of false positive detections by actively using negative samples. The results showed that the proposed R-sGAIA and HBBT significantly improved the F1 score by 5.9% compared to the baseline EfficientDet-D7 + RandAugment (F1: 57.8%, recall: 90.2%, precision: 42.5%). This score is higher than the physician's cancer detection rate, indicating that at least 2 out of 5 areas detected are cancerous, confirming the utility of gastric cancer screening.

INDEX TERMS Gastric cancer, X-ray, screening, data augmentation, negative sample training, computeraided diagnosis.

### I. INTRODUCTION

**▼** ASTRIC cancer is the third most deadly cancer in the world [1]. Advanced gastric cancer has a poor prognosis, but early prognosis before metastasis is good, so early detection and appropriate treatment are important. Gastric cancer is usually diagnosed by endoscopy or radiography. The sensitivity of endoscopy is reported to be 95.4%, which is superior to other methods such as gastric radiography or X-ray at 85.5% [2]. However, endoscopy is not suitable for screening purposes because it can only be performed by a

doctor and the number of people who can be screened is limited. Gastric X-ray, on the other hand, can be performed by radiographers and provides a large number of images, making it suitable for screening. This is the major advantage over endoscopic diagnosis. The images taken are later read by the doctor to diagnose the shape of the stomach and the atrophy of the mucosa membrane [3]-[6]. The problems with this diagnostic method are 1) it is subjective and highly dependent on the reading experience of physician, 2) it has reproducibility problems, 3) it is labor intensive, and 4) it

1

**VOLUME 9, 2021** 

arXiv:2108.08158v2 [eess.IV]



takes time to learn diagnostic techniques compared to other imaging methods (CT, MRI, PET/CT, etc.) [7]. Therefore, there is a need to realize an automatic screening assistance system that can accurately and quickly detect gastric abnormalities from gastric X-ray images in clinical settings.

Healthy gastric folds are thin, smooth, and parallel, but gastric diseases, such as inflammation, infection, ulcers, and tumors, can change the thickness and size of the gastric folds, resulting in irregular bends, depressions, and tears in the lining mucosa [5]. Most of the research on diagnostic support using gastric X-rays is aimed at detecting gastritis, the stage before gastric cancer or the presence of H. pylori infection, which is believed to be the cause of gastric cancer [8]–[18]. Among these proposals, methods based on deep learning represented by convolutional neural networks (CNN) have reported excellent results in the detection of gastritis. The main advantage of these deep learning techniques is that they can automatically capture efficient features for the target task, which is promising for tasks in this area where disease features are difficult to define. However, studies directly detecting gastric cancer from radiographs are very limited, despite the fact that the diagnosis of gastric cancer is much more important in terms of life expectancy. This may be because gastric cancer is more difficult to diagnose, especially in the early stages, compared to gastritis, where the lesion often expands and develops to some degree. It has been reported that it is difficult to distinguish gastritis from gastric cancer even when using the latest machine learning techniques on endoscopic images, where signs of the disease are easily visible [19].

In the field of computer vision research, CNN-based object detection methods (e.g., Faster R-CNN [20], YOLOv3 [21], EfficientDet [22], and YOLOv7 [23]), which can simultaneously detect and classify the location of multiple objects in images have been proposed and widely used. Because these object detection methods can represent the location of the regions involved, they have high explanatory power for the predicted results, as opposed to simply determining benign or malignant on an image-by-image basis. These features are extremely important in medical applications [24]-[28]. In a study of gastric X-ray images, Laddha et al. used YOLOv3 to automatically detect gastric polyps, achieving a mean average precision (mAP) of 0.916 [27]. On the other hand, these object detection methods require annotation of lesion locations prior to training, which is extremely costly. The aforementioned gastritis detection studies [15]-[18] used a patch-based CNN that only needed to be annotated on an image-by-image basis to avoid high annotation costs, while fully understanding the explanatory advantages provided by the object detection model. However, in gastric cancer, where diagnostic difficulties and outcomes are more severe, it is critical that physicians be able to interpret the results of diagnostic support systems.

Based on this, we proposed a diagnostic support system that directly targets gastric cancer using X-ray images, which have rarely been studied, and provides high explanatory

power for the results [28]. Thanks to the proposed stochastic gastric image augmentation (sGAIA) based on medical knowledge, this system was able to represent candidate regions of gastric cancer in a boundary-box with high accuracy. The recall (= sensitivity) and precision of the detected bounding boxes were 92.3% and 32.4%, respectively, in an evaluation using images of patients different from the training set. This is about 7% higher recall than that achieved by doctors (85.5%), and the box-by-box evaluation confirmed that the ratio of true to false detections was 1:3, which is sufficient for practical use. The object detection model trained with the sGAIA has achieved a practical level of accuracy, but further performance improvements are desirable.

Currently, widely-used object detection methods have the disadvantage of not being able to explicitly use negative data for learning, in addition to the high cost of annotation. When such models are used for lesion detection, only images with lesions are used for training; control images without lesions cannot be used. There is much room for improvement here, which is one of the main themes of the work in this paper. When dealing with medical images, data is expensive and we believe that actively using healthy control images that do not contain lesions for training can improve the overall ability of the model to detect lesions. This is equivalent to reducing the cost of annotation to achieve the same performance.

In this paper, we propose a practical gastric cancer screening system. The system includes two new proposals: refined stochastic gastric image augmentation (R-sGAIA), which is an improvement of sGAIA, and hard boundary box training (HBBT), which uses control images that cannot be used for training in the past and includes areas prone to false positive detection in the training. To suppress the high-confidence false positives predicted by the object detector, HBBT registers each of these boxes as a "hard-sample" class, and retrains the model until the predetermined convergence conditions are met. We investigated 4,608 gastric X-ray images obtained from 140 patients in a clinical setting and confirmed the practicality and effectiveness of the proposed system by evaluating the gastric cancer detection performance with a patient-based cross-validation strategy.

The contributions of this study are as follows:

- Proposal of R-sGAIA, a more sophisticated probabilistic augmentation of gastric folds region enhancement based on medical findings.
- Proposal of HBBT, a recursive training strategy with hard sample class assignment for false positive detection that also utilizes control images, which significantly reduces the number of false positives.
- Our gastric cancer screening system based on Efficient-Det with the proposed R-sGAIA and HBBT achieved very practical performance (recall = 90.2%, precision = 42.5%, F1 = 57.8%, 0.51sec/image).

This score is higher than the physician's cancer detection rate and indicates that at least 2 out of 5 areas detected are cancerous.



#### **II. RELATED WORK**

## A. DIAGNOSTIC SUPPORT USING GASTRIC X-RAY IMAGES

In the 1990s, a method for effectively extracting the pattern of gastric folds by applying binarization as a preprocessing step and a method for estimating the gastric region based on the position of the barium reservoir were proposed [8], [9]. In the 2010s, more empirical studies focused on gastric folds began to emerge [10]–[14]. Ishihara et al. calculated numerous statistical features (7,760 per case) for H. pylori infection, a major cause of gastric cancer, by focusing on post-infection mucosal patterns and gastric folds. Their support vector machine based on the data of 2,100 patients, eight per person, yielded a sensitivity (SE) of 89.5% and a specificity (SP) of 89.6% [14].

Recently, taking advantage of deep learning techniques, research has been conducted on the detection of gastritis using patch-based CNN on gastric X-ray images [15]–[18]. Although these methods target gastritis, which is easier to diagnose than gastric cancer, they achieve high detection accuracy and are considered practical in diagnostic assistance. Kanai et al. used a patch-based CNN to detect Helicobacter pylori-associated chronic atrophic gastritis [18]. They trained image patches of the inside and outside of the stomach and made a diagnosis by a majority vote of each estimated result in the stomach region. Manual annotation of regions of interest prior to training and self-learning to increase the number of training patches ultimately yielded a harmonic mean sensitivity and specificity of 95.5% for the test data of different patients.

While excellent screening results have been achieved for gastritis, the detection of more serious and difficult to diagnose gastric cancers has not been well studied. In the case of gastric cancer, it is also important to provide an explanation for the results. The proposed method is a significant improvement of our previous work, a gastric cancer detection system that can present explainable results [28], with two new technical proposals.

## B. DIAGNOSTIC SUPPORT RESEARCH FOR ENDOSCOPIC IMAGES

In recent years, many methods have been proposed to use deep learning technology to analyze narrow-band endoscopy images to assist in the diagnosis of gastric cancer [19], [29]–[31].

Wu et al.'s classic VGG16 or ResNet-50 models achieved an SE of 94.0% and SP of 91.0% based on 24,549 images for diagnosing early gastric cancer [29]. Li et al.'s Inception-v3 model achieved an SE of 91.2% and SP of 90.6% based on 2,429 images of gastric magnification endoscopy with narrow-band imaging [30]. Horiuchi et al. trained GoogLeNet with 1,499 images of gastric cancer and 1,078 images of gastritis images and achieved SE=95.4%, SP=71.0%, AUC=0.852. Although these methods produce excellent results, none of them have statements that clearly separate the training data set from the patients for whom the

images in the evaluation set were taken. In other words, it is possible that the same patient images are mixed in the training and test data. In this case, the test data, which is very close to the training data, is evaluated, resulting in a score that is much higher than the original ability. Kanayama et al. constructed a diagnostic support system using 129,692 gastrointestinal endoscopy images with sophisticated CNNbased networks, including one synthesizer network and two different types of discriminator networks [31]. In this study, the images of the same patient were not divided into training and evaluation sets, i.e., they were evaluated the performance appropriately. They reported an average precision (AP) of 0.596 in cancer detection performance. Although the numerical performance of this method seems inferior, this method is based on a newer and more sophisticated ML model than previously reported methods and is considered to represent a true diagnostic capability for this problem based on current machine learning techniques. They generated 20,000 highresolution lesion images from 1,315 narrow-field-of-view images of the lesion by their own generative adversarial network (GAN) [32], and added these images to the training set. As a result, the AP reported an improvement in cancer detection performance to 0.632.

## III. PRACTICAL GASTRIC CANCER SCREENING SYSTEM

This paper proposes a practical gastric cancer screening system using gastric X-ray images. The system displays suspected cancerous sites with bounding boxes so that physicians can confirm the validity of the estimation. The two technical proposals in this paper significantly improve the performance of the system and achieve practical accuracy. The overall structure of the proposed system is shown in Figure 1. This study has been approved by the Institutional Review Board of Tokai University Hospital (No. 20R-033, date of approval: Jun. 12th, 2020). The main technical proposals are (1) refined stochastic gastric image augmentation (R-sGAIA) for effective detection of gastric fold regions, and (2) hard boundary box training (HBBT) that avoids false positives by assigning "hard sample" classes to the bounding box regions where false positives are detected and iteratively learning them. In this paper, the object detection model used is EfficientDet [22], which uses EfficientNet [33], a CNN with reported excellent performance, as its backbone, but the choice of the model used is arbitrary. The input is 2,048×2,048 pixels, and the output is a bounding box surrounding the presumed cancerous region in the image and its confidence score.

## A. REFINED STOCHASTIC GASTRIC IMAGE AUGMENTATION (R-SGAIA)

The proposed R-sGAIA is a refined version of our previous proposal, sGAIA [28]. The proposed R-sGAIA and sGAIA are probabilistic online data augmentation methods that can generate various images highlighting gastric folds in X-ray images based on medical knowledge to detect inflammation



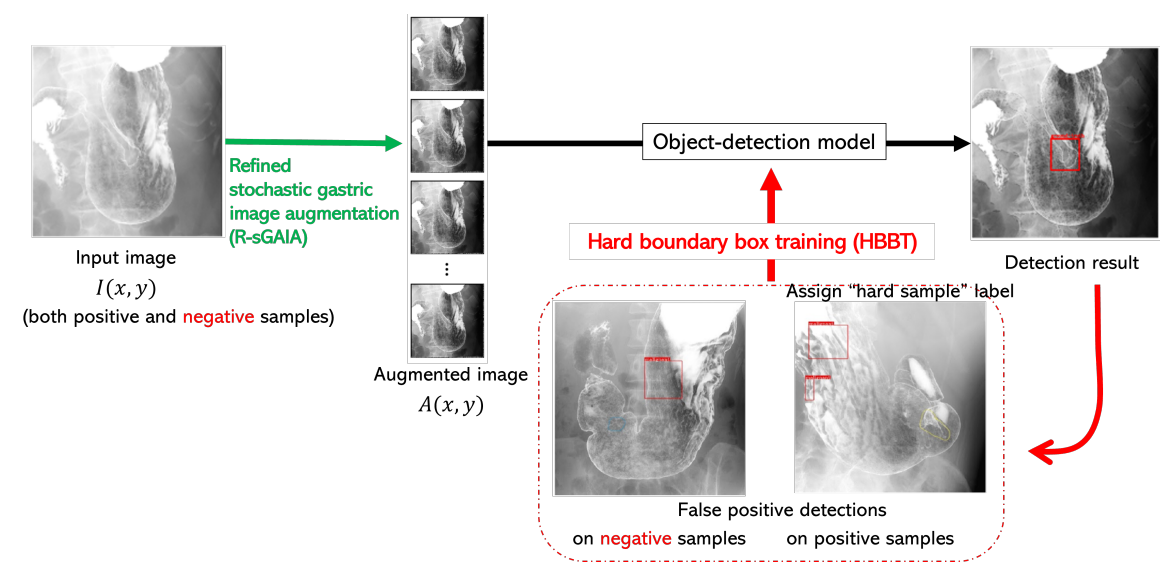


FIGURE 1: Overview of the proposed gastric cancer screening system.

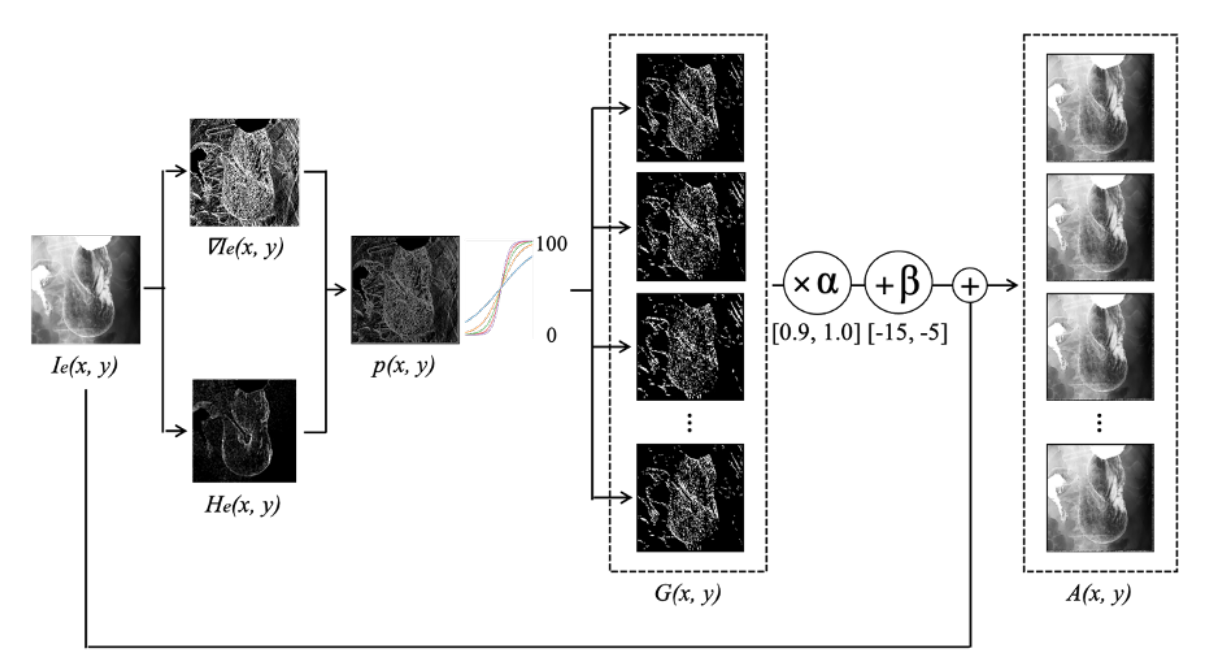


FIGURE 2: Overview of refined stochastic gastric image augmentation (R-sGAIA).

on the gastric mucosal surface. The former sGAIA improved the detection of gastric cancer by 6.9% in terms of the F1-score (recall 92.3%, precision 32.4%) on a Faster R-CNN model with ResNet-101 as the backbone, validating its practical screening performance. However, in the sGAIA, the emphasis probability of each pixel p(x,y), which is important for an effective enhancement, was subjectively determined as a discrete value based on the results of preliminary experiments. In the proposed R-sGAIA, the p(x,y) becomes a flexible continuous function based on only two hyperparameters.

A schematic of the proposed R-sGAIA process is shown

in Figure 2. Like sGAIA, R-sGAIA consists of the following four steps, where only step 2 is different.

• (Step 1) Calculation of edge strength E(x,y) First, a contrast-enhanced image  $I_e(x,y)$  is generated from the original gastric X-ray image I(x,y) by histogram equalization. Then, its gradient and high-frequency components,  $\nabla I_e(x,y)$ , and  $H_e(x,y)$ , are obtained using general image processing techniques such as Canny edge detection filter and Butterworth high-pass filter, respectively. Each of them is normalized to [0,1], and the normalized edge strength E(x,y) is calculated as follows.



$$E(x,y) = (\overline{\nabla I_e(x,y)} + \overline{H_e(x,y)})/2.$$
 (1)

,where  $\overline{v(x,y)}$  is the linearly normalized value of v(x,y) to [0,1].

• (Step 2) Calculation of the probability of a gastric fold region p(x, y)

The area of the edge of the gastric folds that is subject to augmentation is determined for each pixel as its probability p(x,y). The proposed R-sGAIA differs from sGAIA in this step. In R-sGAIA, the edge intensity e=E(x,y) of each pixel is used to obtain a probability map p(x,y) of the gastric folds and edges using probabilities based on the sigmoid function defined below.

$$p(x,y) = p(e) = p(E(x,y))$$
  
=  $\frac{1}{1 + \exp(-\gamma(E(x,y) + \theta))}$ . (2)

The parameters  $\gamma$  and  $\theta$  are hyperparameters, respectively, defining the slope of the sigmoid function and adjusting the probability of running the augmentation of E(x,y) to be 50%. They were determined based on the diagnostic performance of the validation data, described below. Figure 3 compares the enhancement selection probability p(e=E(x,y)) based on the feature intensity e for R-sGAIA and sGAIA. Note that, in sGAIA, the probability p(e) is subjectively determined based on preliminary experiments, as described above.

- (Step 3) Determination of gastric fold edge region G(x, y)
   According to the probability map P(x, y), a binary mask G(x, y) of the gastric fold regions to be enhanced is determined by pixel-by-pixel sampling. Since this result is noisy, a morphological open operation is performed to remove many small isolated regions. G(x, y) is created in such a way that a different mask is generated for each trial. This is the key to generating enhanced images of different gastric folds.
- (Step 4) Generation of enhanced gastric fold images A(x,y)Finally, an enhanced gastric fold edge image A(x,y) is obtained as follows:

$$A(x,y) = I_e(x,y) + \alpha G(x,y) + \beta. \tag{3}$$

Here,  $\alpha$  and  $\beta$  are augmented parameters. The value of  $\alpha$  ranges from 0.9 to 1.0 and that of  $\beta$  ranges from -15 to -5, and they are chosen randomly for each processing. Based on this, the proposed R-sGAIA probabilistically enhances the location and intensity of the gastric fold region each time. Thus, it produces a different enhanced gastric image for each trial and is highly compatible with online data augmentation in deep neural network training. Another significant advantage of the proposed R-sGAIA is that it does not require any additional runtime.

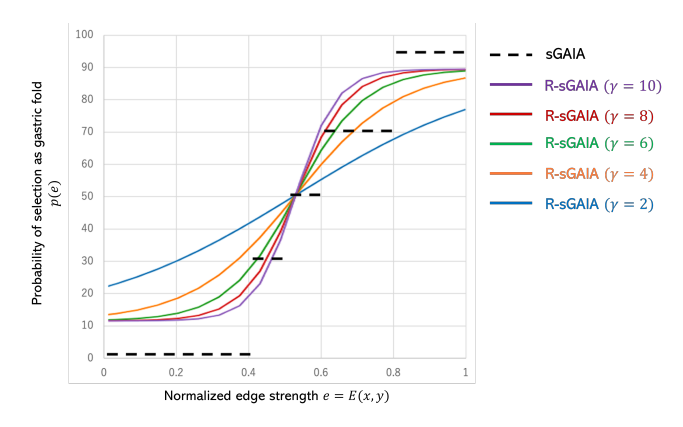


FIGURE 3: Probability of being detected as a gastric fold edge to be highlighted.

#### B. HARD BOUNDARY BOX TRAINING (HBBT)

The diagnostic support system for gastric X-ray images is a one-class detection problem that targets only positive (i.e., malignant) regions. However, our task has many regions with similar image features, making them difficult to discriminate even for experts. Given a very large number of training images, the recently developed deep learning-based object detection algorithms can achieve the desired detection performance for the task, but this is difficult in situations where the labeled supervisory data is limited. The images in Figure 4 are typical false positives indicated by experts in the experiments conducted using a vanilla detection model (i.e., EfficientDet-D7 without the proposed HBBT). The results show that most of these false positives fall broadly into the five categories shown in examples (b)-(f) in Figure 4. However, it is difficult to clearly define and control these features in advance.

Especially in a fine-grained task like our current goal, it is very important to reduce such hard negatives that have high image similarity but are not the target. As described above, various training techniques, including adversarial learning, have been applied in general recognition problems to reduce the number of hard negatives and increase the generalizability of the models, but their application to object detection models is not common.

In fact, as mentioned earlier, the biggest room for improvement in object detection models is the active use of negative samples, i.e., healthy controls. Conventional object detection algorithms based on deep learning only use images in which there is an object to be detected, and control cases without an object to be detected cannot be included in the training. This is a very wasteful situation. Therefore, we propose HBBT, which is a very simple and effective way to suppress false positives by referring to self-training and the concept of Adaboost [34]. In general, training negative samples, which are more prone to false positives among the training data, is effective in constructing detectors with few false positives. In our HBBT, we call the false-positive boundary boxes detected by the model hard boundary boxes,



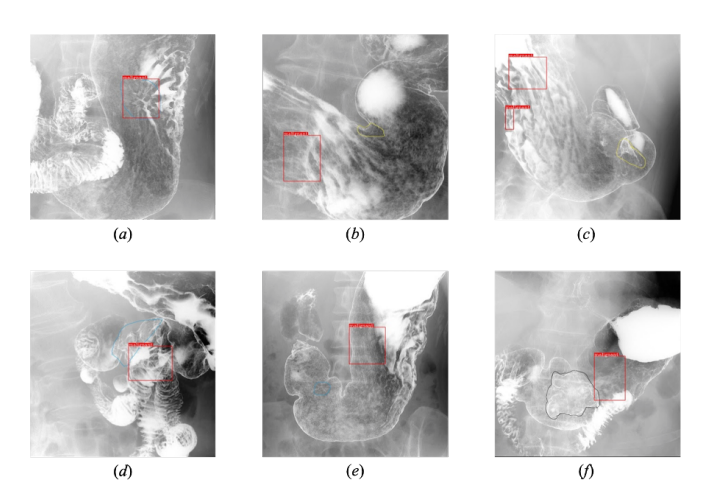


FIGURE 4: Positive example and five typical false positives provided by experts.

(a) Positive example. (b) The area overlapping the osteophytes and spinous processes of the vertebral body. (c) Area where folds are gathered due to lack of air in the stomach. (d) Area where the duodenal Kerckring's folds overlap with the stomach. (e) Areas where the mucosal surface of the stomach is irregular due to chronic gastritis. (f) Areas of advanced cancer that appear as wall changes rather than masses.

assign a hard-sample label to them, and train the model as a two-class detection problem. This newly added hard-sample class label is treated as a negative example. Training is repeated until an optimal F1-score is obtained from the validation data. The important point here is that not only positive data (e.g. with cancerous regions), which can be used for normal training, but also negative (i.e., healthy, control) data, which are generally available in large quantities, can be used to detect hard boundary boxes, i.e. can be used for training.

#### **IV. EXPERIMENTS**

#### A. DATASETS

The image set used in this study consisted of 4,724 gastric X-ray images (1,117 images with 1,504 lesion annotations by radiologists and 3,607 images without lesions) from 145 patients in clinical settings provided by Tokai University School of Medicine, Japan. A total of 116 images from five randomly selected patients (49 of them with 49 annotated boxes) were used as validation data to determine the hyper parameters and the decision to terminate HBBT, and the remaining 4,608 images from 140 patients were used to train and evaluate the proposed system.

Each image was in 8-bit grayscale and had a resolution of  $2,048 \times 2,048$  pixels. Based on each expert annotation of the gastric cancer locations, the smallest rectangle surrounding each location was defined as a bounding box to be detected. A patient-based five-group cross-validation was used for training and evaluation. Precision, recall, and F1-score were used as the performance indicators of this system.

TABLE 1: Detection performance in validation images for determining hyperparameter  $\gamma$ .

$\gamma$	precision	recall	F1-score
2	35.7	89.6	51.1
4	39.6	91.7	55.3
6	31.2	91.7	46.6
8	32.8	89.6	48.0
10	30.3	89.6	45.3

The system provided candidate lesion bounding boxes and their associated confidence scores were above a predefined detection threshold  $\xi$ .

#### B. DETAILS OF THE DETECTION MODEL

We used EfficientDet-D7 as a gastric cancer detection model with an input resolution of  $1,536 \times 1,536$  pixels. One difference from the original image size was the margin for random cropping performed during training. This model used EfficientNet-B7 as the backbone (384 channels in the feature map, eight layers of BiFPN, and five layers of classification/rectangle heads). The learning rate was 0.001, the batch size was 32, and the number of trainings was 100. The optimization method used was momentum SGD [35], and the exponential decay rate of the first-order moment was set to 0.9. To build a robust lesion detector with respect to different lesion sizes, shapes, and resolutions, we used RandAugment [36], which is one of the state-of-the-art data augmentation methods that randomly applies 14 types of data augmentation, excluding color augmentation, to the training data, and treated the model as a baseline for performance.

#### C. EXPERIMENTAL CONDITIONS

### 1) Determination of hyperparameters in R-sGAIA

In this section, we describe the hyperparameters  $\theta$  and  $\gamma$  of the proposed R-sGAIA.  $\theta$  is a hyperparameter that determines the edge strength E(x,y) for which the probability of being considered a gastric fold is 50% in the sigmoid function p(e=E(x,y)), and was determined to be 0.55 based on the distribution of validation results. For  $\gamma$ , which characterizes the slope of p(e), we selected  $\gamma=4$  from 2, 4, 6, 8, and 10 (Table 1) from the detection performance on validation images.

### 2) Detection of suspicious cancerous regions

To confirm the effectiveness of the proposed system with RsGAIA and HBBT, we conducted comparative experiments using the following combinations of conditions. Since there is no directly comparable literature on gastric cancer detection, we implemented Laddha et al.'s method [27] based on YOLO-v3 and compared the performance on our task.

#### • Model selection

We selected two object detection models for this task: ResNet-101+Faster R-CNN (model 1) and EfficientDet-D7 (model 2). The first model has been widely used in the literature including sGAIA. The second model is











FIGURE 5: Example of augmented images (leftmost: original, others: enhanced images with R-sGAIA.

one of the most advanced object detection models used in many studies, although newer models are currently being proposed. We applied RandAugment [36] as an online data augmentation to the model and used it as the baseline for each model (i.e., baseline model 1 and 2, respectively). Since this task involved a grayscale image, we omitted the color augmentation. Based on the detection performance of the validation dataset, we selected four types of augmentation out of 13, with an intensity level of 3 (i.e., M=4 and N=3 according to their notation).

Comprehensive evaluation of the proposals
 We compared the performance of each model with
 and without the proposed technique. Regarding data
 augmentation, we chose either RandAugment, conventional sGAIA (+sGAIA), or the proposed R-sGAIA
 (+R-sGAIA). Regarding the proposed HBBT, this was
 annotated as use (+HBBT) or not.

#### **V. RESULTS**

Figure 5 shows an example of the augmented image obtained with the proposed R-sGAIA for the leftmost original image. Figure 6 shows an example of the comparison of cancer detection on the EfficientDet-D7 network (baseline model 2) with and without the proposed R-sGAIA and HBBT. Here are the input images (a), the detection results with RandAugment (b), and those with the proposed R-sGAIA+HBBT (c). The proposed system (c) can correctly detect the gastric cancer region without being affected by the unevenness of the mucosa, and small areas as shown in the top and middle rows, respectively. In contrast, as shown in the bottom row, the result almost covers the ROI, but is misaligned, so we evaluate it as a false-positive.

The detection performance of gastric cancer regions from gastric X-ray images is summarized in Table 2. In this experiment, the detection threshold  $\xi$  of the bounding box is determined such that the sensitivity of detecting gastric cancer is about 90%, which is higher than the doctor's 85.5%. Our system using the proposed techniques, R-sGAIA and HBBT, achieved recall of 90.2%, precision of 42.5%, and F1-score of 57.8% (Table 2). We confirmed that each of the proposed R-sGAIA and HBBT improved the cancer detection performance for both baseline models and outperformed the

previously proposed method. The processing time required to process one X-ray image is approximately 0.512 sec, which makes the proposed system suitable as a practical screening system for gastric X-ray images.

#### VI. DISCUSSION

The obtained cancer detection performance is significantly better than those achieved with the baseline methods, including RandAugment; a state-of-the-art general data augmentation strategy, as well as the existing methods (i.e., sGAIA and those proposed by Laddha et al.). The ability of the proposed system to detect cancer was higher than that of the physician's reading ( $\sim$ 85.5%), and in terms of percentage, more than two out of five detection results presented by the system were related to cancer, indicating that the system is practical enough for on-site screening and puts little burden on doctors. Since recall (= sensitivity) and precision in detection have a trade-off relationship, if detection sensitivity is kept constant at a higher level than the target, improved performance will lead to improved precision. This means that the number of points to be checked by the doctor is reduced, i.e. the burden is reduced.

#### A. R-SGAIA

The proposed R-sGAIA can probabilistically highlight the gastric folds on a pixel-by-pixel basis based on the medical findings, as shown in Figure 5. In this experiment, we found that the proposed R-sGAIA achieved 6.0% and 2.7% better performance in terms of the F1-score than RandAugment on baseline models 1 and 2, respectively. This confirms the importance of our probabilistic augmentation based on medical knowledge. On baseline 2, R-sGAIA further improves the F1-score by 1.2% over the previous sGAIA in a stand-alone comparison. This may be because R-sGAIA used validation data to determine p(e) as a continuous function, and was thus able to generate many types of enhancement images that better enhanced the gastric folds than sGAIA, which used a subjectively fixed value. The fact that the function of p(e) with respect to the edge strength e = E(x,y) is approximately between 0.1 and 0.9 is thought to have contributed to the performance improvement by allowing more stochastic variation than sGAIA in the very strong and weak



model		augmentation			HBBT	precision	recall	F1-score
model 1	model 2	RandAug †	sGAIA	R-sGAIA		precision	recall	1-1-score
						26.5	89.7	40.9
			•			•		
✓		✓				28.4	90.1	43.2
<b>√</b>			<b>√</b>			33.8	90.4	49.2
✓				<b>√</b>	✓	38.7	90.1	54.1
	<b>√</b>	✓				36.4	90.5	51.9
	<b>√</b>		✓			37.9	90.1	53.4
	<b>√</b>			✓		39.2	90.2	54.6
	<b>√</b>	<b>√</b>			<b>√</b>	39.4	89.9	54.8
	<b>√</b>			✓	<b>√</b>	42.5	90.2	57.8
							model 2   RandAug †   sGAIA   R-sGAIA     Precision	model 1   model 2   RandAug †   sGAIA   R-sGAIA     precision   recall

TABLE 2: Comparison of detectability of gastric cancer sites

edge strength regions, i.e., by contributing to the diversity of the generated images.

#### B. HBBT

The proposed HBBT is a new and effective learning method that actively uses negative samples, in this case images of healthy controls, which cannot be used for training by conventional object detection models. Although the HBBT is a very simple method that recursively learns to eliminate false positives detected on images including control images, it alone improves the F1 score by 4.9% and 2.9% on baseline models 1 and 2, respectively. The HBBT is a general-purpose learning method that can be combined with any object detection algorithm, not just gastric cancer detection as in this case. Since the final model detection is determined by the bounding box confidence threshold, HBBT not only reduces the number of false positives, but also the number of false negatives (middle case in Figure 6). When combined with R-sGAIA, it achieves a large improvement of +10.9% for baseline 1 and +5.9% for baseline 2.

#### C. FOR PRACTICAL SCREENING

Since R-sGAIA is an online data augmentation method and HBBT is a training method, they do not affect the execution time of the inspection. The processing time of 0.5 seconds per image under current conditions is considered sufficiently practical, and further improvement of the detection model is expected to increase the speed in the future.

The detection of a gastric cancer region from the X-ray images is inherently difficult, not only for automatic diagnosis systems but also for experts. Despite these difficulties, our system achieves a significant improvement in detection performance. The final result of 42.5% precision at 90.2% recall is considered sufficient for screening, but there is still room for improvement. In the future, we would like to examine the results more closely with the help of experts to further improve the system further.

#### VII. CONCLUSIONS

This paper proposes a practical screening system for gastric cancer from X-ray images by using the following two proposed methods: (1) R-sGAIA and (2) HBBT. The detection performance of the proposed system (R-sGAIA + HBBT on EfficientDet-D7 network) was 90.2% for recall and 42.5% for precision, which showed a 5.9% improvement in F1-score compared to the same network with RandAugment, which is a state-of-the-art augmentation method. This result can be attributed to the fact that R-sGAIA was able to obtain more effective probabilities for highlighting gastric folds than the conventional sGAIA or RandAugment, and that HBBT was able to explicitly learn negative samples (i.e., healthy controls), which it has not been able to utilize in the past. As R-sGAIA is an online data augmentation method and HBBT is a learning method, they do not affect the execution time of the examination and are therefore useful screening systems for gastric X-ray images.

#### **REFERENCES**

- P. Rawla and A. Barsouk, "Epidemiology of gastric cancer: global trends, risk factors and prevention," Przeglad Gastroenterol., vol. 14, no. 1, pp. 26-38, 2019
- [2] C. Hamashima, M. Okamoto, M. Shabana, et al., "Sensitivity of endoscopic screening for gastric cancer by the incidence method," International Journal of Cancer, vol. 133, no. 3, pp. 653-659, 2013.
- [3] N. Uemura, S. Okamoto, S. Yamamoto, et al., "Helicobacter pylori infection and the development of gastric cancer," New England Journal of Medicine, vol. 345, pp. 784-789, 2001.
- [4] D. M. Roder, "The epidemiology of gastric cancer," Gastric Cancer, vol. 5, pp. 5-11, 2002.
- [5] P. Correa, M. B. Piazuelo, and M. C. Camargo, "The future of gastric cancer prevention," Gastric Cancer, vol. 7, no. 1, pp. 9-16, 2004.
- [6] Quality Control Committee for Gastric Cancer Screening in the Japanese Society of Gastrointestinal Cancer Screening, "Atras for Classifying Diagnoses in Gastric X-ray Photography," Nankodo, 2017.
- [7] M. Nagai, Y. Yamada, S. Nakamura, H. Azuma, and A. Fujinaga, "An Attempt to unify the expression of reading X-rays in the stomach health checkup Development and evaluation of Reading supporting tool Ver. 1 -," Journal of Gastroenterological Cancer Screening, vol. 47, no. 4, pp. 450-462, 2009.
- [8] J. Cooper, G. Khan, G. Taylor, I. Tickle, and T. Blundell, "X-ray analyses of aspartic proteinases: Ii. three-dimensional structure of the hexagonal crystal form of porcine pepsin at 2.3 a resolution," Journal of Molecular Biology, vol. 214, no. 1, pp. 199-222, 1990.

<sup>\* (</sup>reference result) originally used for gastric polyp detection with YOLOv3.

<sup>&</sup>lt;sup>†</sup> RandAugment [36] with M = 4 and N = 3.



- [9] Y. Kita, "Model-driven contour extraction for physically deformed objectsapplication to analysis of stomach x-ray images," International Conference on Pattern Recognition, pp. 280-284, 1992.
- [10] N. Nagano, T. Matsuo, "Computer-aided diagnosis of gastrointestinal radiographs using adaptive differential filter and level set method," International Conference on Modelling, Identification and Control, pp. 442-447, 2010.
- [11] T. Minemoto, S. Odama, A. Saitoh, T. Isokawa, N. Kamiura, H. Nishimura, S. Ono, and N. Matsui, "Detection of tumors on stomach wall in x-ray images," International Conference on Fuzzy Systems (FUZZ), pp. 1-5, 2010.
- [12] K. Abe, H. Nakagawa, M. Minami, and H. Tian, "Features for discriminating normal cases in mass screening for gastric cancer with double contrast x-ray images of stomach," Journal of Biomedical Engineering and Medical Imaging, vol. 1, no. 6, 2014.
- [13] K. Ishihara, T. Ogawa and M. Haseyama, "Helicobacter pylori infection detection from multiple X-ray images based on decision level fusion," IEEE International Conference on Image Processing (ICIP), pp. 2769-2773, 2014.
- [14] K. Ishihara, T. Ogawa, and M. Haseyama, "Helicobacter pylori infection detection from multiple x-ray images based on combination use of support vector machine and multiple kernel learning," IEEE International Conference on Image Processing (ICIP), pp. 4728-4732, 2015.
- [15] K. Ishihara, T. Ogawa, and M. Haseyama, "Detection of gastric cancer risk from x-ray images via patch-based convolutional neural network," IEEE International Conference on Image Processing (ICIP), pp. 2055-2059, 2017.
- [16] M. Kanai, R. Togo, T. Ogawa and M. Haseyama, "Gastritis Detection from Gastric X-Ray Images Via Fine-Tuning of Patch-Based Deep Convolutional Neural Network," IEEE International Conference on Image Processing (ICIP), pp. 1371-1375, 2019.
- [17] R. Togo, N. Yamamichi, K. Mabe, Y Takahashi, C. Takeuchi, M. Kato, N. Sakamoto, K. Ishihara, T. Ogawa, and M. Haseyama, "Detection of gastritis by a deep convolutional neural network from double-contrast upper gastrointestinal barium X-ray radiography," Journal of Gastroenterology, vol. 54, no. 4, pp. 321-329, 2019.
- [18] M. Kanai, R. Togo, T. Ogawa, and M. Haseyama, "Chronic atrophic gastritis detection with a convolutional neural network considering stomach regions," World Journal of Gastroenterology, vol. 26, no. 25, pp. 3650-3559, 2020.
- [19] Y. Horiuchi, K. Aoyama, Y. Tokai, T. Hirasawa, S. Yoshimizu, A. Ishiyama, et. al, "Convolutional neural network for differentiating gastric cancer from gastritis using magnified endoscopy with narrow band imaging," Digestive Diseases and Sciences, Vol. 65, No. 5, pp.1355-1363, 2020.
- [20] S. Ren, K. He, R. Girshick, and J. Sun, "Faster R-CNN: towards real-time object detection with region proposal networks," Neural Information Processing Systems (NIPS), vol. 1, pp. 91-99, 2015.
- [21] J. Redmon, and A. Farhadi, "YOLOv3: An incremental improvement," arXiv:1804.02767, 2018.
- [22] M. Tan, R. Pang, and Q. V. Le, "EfficientDet: Scalable and efficient object detection," IEEE Conference on Computer Vision and Pattern Recognition (CVPR), 2020.
- [23] C.Y Wang, A. Bochkovskiy, H.Y.M. Liao, "Yolo7: Trainable bag-of-freebies sets new state-of-the-art for real-time object detectors," arXiv preprint 2207.02696, 2022.
- [24] Z. Li, C. Wang, M. Han, Y. Xue, W. Wei, L. Li, and F. Li, "Thoracic disease identification and localization with limited supervision," IEEE Conference on Computer Vision and Pattern Recognition (CVPR), 2018.
- [25] T. Hirasawa, K. Aoyama, T. Tanimoto, et al., "Application of artificial intelligence using a convolutional neural network for detecting gastric cancer in endoscopic images," Gastric Cancer, vol. 21, pp. 653-660, 2018.
- [26] Z. Zhang, Y. Guo, Y. Lu, and S. Li, "Detection of metastatic lymph nodules in gastric cancer using deep convolutional neural networks," IEEE/ASME (AIM) International Conference on Advanced Intelligent Mechatronics, 2019
- [27] M. Laddha, S. Jindal, and J. Wojciechowski, "Gastric polyp detection using deep convolutional neural network," Proceedings of the 2019 4th International Conference on Biomedical Imaging, Signal Processing, pp. 55-59, 2019.
- [28] H. Okamoto, Q. H. Cap, T. Nomura, H. Iyatomi, and J. Hashimoto, "Stochastic gastric image augmentation for cancer detection from X-ray Images," IEEE International Conference on Big Data, pp. 4858-4663, 2019.

- [29] L. Wu, W. Zhou, X. Wan, et al., "A deep neural network improves endoscopic detection of early gastric cancer without blind spots," Endoscopy, vol. 51, pp. 522-531, 2019.
- [30] L. Li, Y. Chen, Z. Shen, et al., "Convolutional neural network for the diagnosis of early gastric cancer based on magnifying narrow band imaging," Gastric Cancer, vol. 23, pp. 126-132, 2020.
- [31] T. Kanayama, Y. Kurose, K. Tanaka, K. Aida, S. Satoh, M. Kitsuregawa, and T. Harada, "Gastric cancer detection from endoscopic images using synthesis by GAN," International Conference on Medical Image Computing and Computer-Assisted Intervention, pp. 530-538, 2019.
- [32] I. Goodfellow, J. Pouget-Abadie, M. Mirza, B. Xu, D. Warde-Farley, S. Ozair, A. Courville, and Y. Bengio, "Generative adversarial nets," Neural Information Processing Systems (NIPS), vol. 2, pp. 2672-2680, 2014.
- [33] M. Tan, and Q. V. Le, "EfficientNet: Rethinking model scaling for convolutional neural networks," IEEE Conference on Computer Vision and Pattern Recognition (CVPR), 2019.
- [34] Y. Freund, R. E. Schapire, "A decision-theoretic generalization of on-line learning and an application to boosting," Journal of Computer and System Sciences, vol. 55, pp. 119-139, 1997.
- [35] N. Qian, "On the momentum term in gradient descent learning algorithms," Neural Networks, vol. 12, no. 1, pp. 145-151, 1999.
- [36] E. D. Cubuk, B. Zoph, J. Shlens, and Q. V. Le, "RandAugment: Practical automated data augmentation with a reduced search space," IEEE Conference on Computer Vision and Pattern Recognition (CVPR) Workshops, 2020

. . .



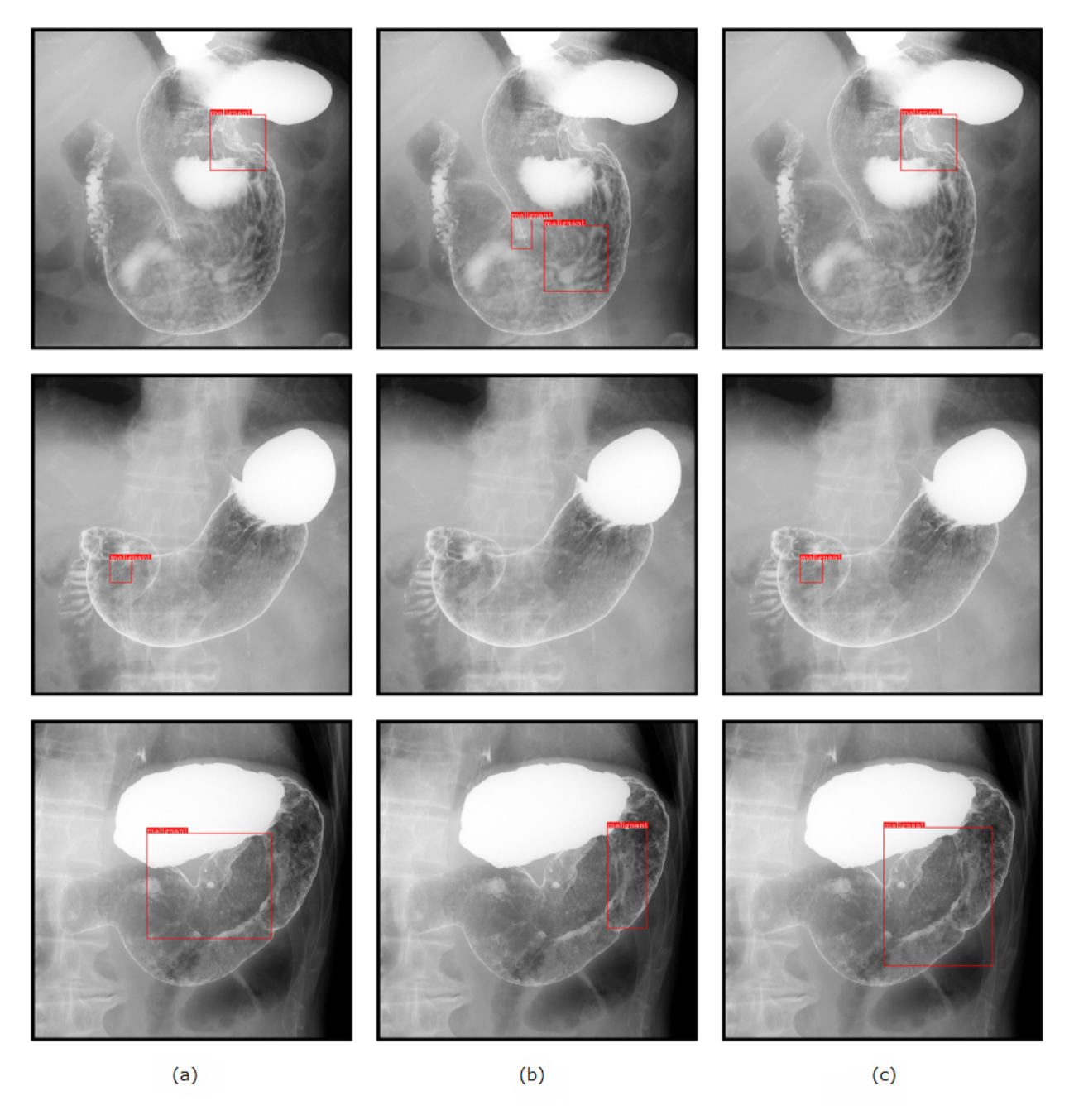


FIGURE 6: Example of cancer detection on EfficientDet-D7 networks: (a) ground-truth region, (b) results obtained with RandAugment (baseline model 2), and (c) those with R-sGAIA+HBBT (proposed). The proposed R-sGAIA+HBBT led to the correct detection for the top and middle examples, whereas the bottom result showed some improvement but was not a correct detection.





HIDEAKI OKAMOTO received his B.E. and M.E. degrees in Applied Informatics from Hosei University, Tokyo Japan, in 2019 and 2021 respectively. His research interests include machine learning and medical image analysis. He is currently working as a machine learning engineer at SoftBank, Corp.



HITOSHI IYATOMI (M'05) received his B.E., M.E. and Ph.D (engineering) degrees form Keio University, Japan in 1998, 2000, and 2004, respectively. During 2000-2004, he worked as a technical consultant at Hewlett-Packard Japan. He joined Hosei University as a research associate in 2004. In 2011, he earned his second Ph.D degree (medical science) from Tokyo Women's Medical University. In 2016-2017, he was a visiting scholar at Johns Hopkins University. He is currently a

professor in the Department of Applied Informatics at Hosei University. He has authored and co-authored more than 140 peer-reviewed journal and conference papers in various research areas based on machine learning such as computer vision, medical applications and natural language processing.

. . .



TAKAKIYO NOMURA received his M.D. and Ph.D.degrees both from Keio University School of Medicine, Tokyo, Japan in 2020. His research interests include visualization of thoracic duct using MRI. He is currently working as a radiologist at Tokai University Hospital.



KAZUHITO NABESHIMA received his M.D. and Ph.D. degrees both from Keio University School of Medicine, Tokyo, Japan in 2011. His research interests include Improvement of surgical technique for gastric cancer and GIST. He is currently working as a surgeon at Tokai University Hospital.



JUN HASHIMOTO received his M.D. and Ph.D. degrees both from Keio University School of Medicine, Tokyo, Japan in 1998. His major is nuclear medicine especially in the fields of nuclear cardiology and neurology. During 1999-2009, he worked as an assistant professor in the Department of Radiology, Keio University School of Medicine. In 2001, he stayed in Hammersmith Hospital, Imperial College, London, UK to learn cardiac PET examinations. In 2009, he moved to

Tokai University School of Medicine, Isehara, Japan as an associate professor, and was promoted to a professor in 2014. He became a board member of the Japanese Society of Nuclear Medicine (JSNM) and the Japanese Society of Nuclear Cardiology (JSNC) in 2015 and 2018, respectively.